General Disclaimer

One or more of the Following Statements may affect this Document

- This document has been reproduced from the best copy furnished by the organizational source. It is being released in the interest of making available as much information as possible.

- This document may contain data, which exceeds the sheet parameters. It was furnished in this condition by the organizational source and is the best copy available.

- This document may contain tone-on-tone or color graphs, charts and/or pictures, which have been reproduced in black and white.

- This document is paginated as submitted by the original source.

- Portions of this document are not fully legible due to the historical nature of some of the material. However, it is the best reproduction available from the original submission.

NASA

Technical Memorandum 79705

The Effects of Ground Hydrology on Climate Sensitivity to Solar Constant Variations

Shu-Hsien Chou, Robert J. Curran and George Ohring

JANUARY 1979

National Aeronautics and
Space Administration

Goddard Space Flight Center
Greenbelt, Maryland 20771

TM79705

THE EFFECTS OF GROUND HYDROLOGY ON CLIMATE SENSITIVITY TO SOLAR CONSTANT VARIATIONS

by

Shu-Hsien Chou

Computer Sciences Corporation

Silver Spring, MD 20910

Robert J. Curran

Laboratory for Atmospheric Sciences

Goddard Space Flight Center

Greenbelt, MD 20771

and

George Ohring

Department of Geophysics and Planetary Sciences

Tel-Aviv University

Ramat-Aviv, Israel

January 1979

GODDARD SPACE FLIGHT CENTER

Greenbelt, Maryland

THE EFFECTS OF GROUND HYDROLOGY ON CLIMATE SENSITIVITY TO SOLAR CONSTANT VARIATIONS

by

Shu-Hsien Chou
Computer Sciences Corporation
Silver Spring, MD 20910

Robert J. Curran
Laboratory for Atmospheric Sciences
Goddard Space Flight Center
Greenbelt, MD 20771

and

George Ohring
Department of Geophysics and Planetary Sciences
Tel-Aviv University
Ramat-Aviv, Israel

ABSTRACT

The effects of two different evaporation parameterizations on the climate sensitivity to solar constant variations are investigated by using a zonally averaged climate model. The model is based on the two-level quasi-geostrophic zonally averaged annual mean model of Ohring and Adler (1978) with some modifications to the heating parameterizations. One of the evaporation parameterizations tested is a nonlinear formulation with the Bowen ratio determined by the predicted vertical temperature and humidity gradients near the earth's surface (model A). The other is the linear formulation of Saltzman (1968) with the Bowen ratio essentially determined by the prescribed linear coefficient (model B).

The computed climates are in good agreement between model A and model B, except for the energy partition between sensible and latent heat at the earth's surface. The simulated temperatures and the radiation quantities at the top of the atmosphere for both models are in good

agreement with the observations, but, the energy partitions between the atmosphere and the earth's surface are different. Compared to the results of Hoyt (1976), the solar heating and the long-wave cooling in the model atmospheres are too small, and the net solar and the net long-wave radiation at the model earth's surfaces are too large. As a result, the turbulent heat flux is too large. The neglect of short-wave absorption by CO_2, O_2, dust, and cloud droplets is responsible for this discrepancy.

The difference in evaporation parameterizations causes a discrepancy in the response of temperature lapse rate to solar constant variations and a difference in the sensitivity of longwave radiation to surface temperature. Compared to the linear evaporation formulation (model B), the nonlinear evaporation formulation (model A) appears to produce a reduction not only in the sensitivity of surface temperature to solar constant variations but also in the amplification of the global climate sensitivity due to ice-albedo feedback. The difference in evaporation also causes a difference in the response of surface heat budget to solar constant variations. The latent and sensible heat fluxes are found to change in the opposite direction in model A, but in the same direction in model B. The results of model A are qualitatively in agreement with those of Wetherald and Manabe (1975).

CONTENTS

THE EFFECTS OF GROUND HYDROLOGY ON CLIMATE SENSITIVITY TO SOLAR CONSTANT VARIATIONS

1. Introduction

The transfer of latent heat from the earth's surface to the atmosphere is an important physical process. It is directly related to the determination of the surface temperature through the surface energy balance equation. It affects indirectly the latent heat release, cloud cover, temperature lapse rate and other dynamics. Charney et al. (1975) adopted two different evaporation parameterizations in the Goddard Institute for Space Studies (GISS) general circulation model (GCM), and found that the difference in evaporation markedly affected cloud cover, precipitation, surface temperature, dynamical instabilities and related eddy activities. The purpose of this study is to investigate the effects of two different evaporation parameterizations on climate sensitivity to solar constant variations using a zonally averaged climate model.

The model is based on the annual mean zonally averaged climate model of Ohring and Adler (1978), hereafter referred to as O/A, with some modifications to the heating parameterizations. For the calculation of evaporation, O/A adopted the linear formulation of Saltzman (1968), in which a linear relationship between latent (evaporation) and sensible heat fluxes at the earth's surface was assumed. According to this parameterization, the Bowen ratio (ratio of sensible to latent heat) is not sensitive to the variation in surface temperature. Also, the changes of sensible and latent heat fluxes resulting from a climate variation are generally in the same direction, and the ratio of the changes is essentially fixed by the prescribed linear coefficient. However, from the GCM numerical experiments, Wetherald and Manabe (1975), hereafter referred to as W/M, found that the Bowen ratio had a strong dependence on surface temperature, and that the changes of these two fluxes due to the variation in solar constant were in the opposite directions. In this study, we have included a simple boundary layer to one of the models to improve the parameterization of evaporation. With this simple boundary layer, the Bowen ratio can be determined from

the vertical gradients of water vapor and temperature near the earth's surface, and the relationship between sensible and latent heat is nonlinear. The responses of the two models, with linear and nonlinear evaporation formulations, to the changes in solar constant are studied. The model with nonlinear evaporation formulation is referred to as model A, and that with the same linear formulation as O/A is referred to as model B.

In section 2, we briefly describe the dynamical model and heating processes with more detail discussion on the model modifications to O/A. In section 3, we examine the performance of both models A and B by comparing the computed climates with the observations. The effects of these two different evaporation parameterizations on the climate sensitivity to solar constant variations are investigated in section 4. Finally, conclusions of the major results of this study are given in section 5.

2. Descriptions of the climate models

It is well known that one of the most difficult problems for a zonally averaged climate model is to parameterize the large-scale eddy transport processes, especially the angular momentum transport. Green (1970) suggested that the angular momentum transport can be parameterized by considering the potential vorticity transport. Following this idea Wiin-Nielsen and Sela (1971) studied the potential vorticity transport and determined the exchange coefficients from the observed atmospheric data. Sela and Wiin-Nielsen (1971), and Wiin-Nielsen and Fuenzalida (1975) incorporated those exchange coefficients into the two-level quasi-geostrophic models to simulate the seasonal variations. Radiative heating is crucially important for climate studies, but has been highly simplified in the aforementioned works. Ohring and Adler (1978) developed an annual mean zonally averaged hemisphere model for climate sensitivity studies using the same dynamic model, but with improved treatments of solar and longwave radiation.

As mentioned in the introduction, two evaporation parameterizations, designated as model A and model B, have been used in this study to investigate the effects of ground hydrology on

the climate sensitivity to solar constant variations. The only difference between them is the treatment of evaporation and convection. Both models are based on O/A with some changes in the heating parameterizations. The difference between model A and O/A is the parameterizations of evaporation, convection, latent heat release, cloud and surface albedo. Since the parts of the model common to O/A have been discussed by Ohring and Adler (1978), they are only briefly described here. Table 1 shows the dynamical model, heating processes, and the methods of computation. The dynamical model is the standard two-level quasi-geostrophic model, with the atmosphere divided into two layers, 0-500mb and 500-1000mb. The governing equations are the zonally averaged quasi-geostrophic potential vorticity equations, which can be obtained by combing the vorticity equation and the thermodynamic energy equation (Sela and Wiin-Nielsen, 1971; Wiin-Nielsen and Fuenzalida, 1975). The 500mb temperatures are computed from the potential vorticity equations, and the surface temperatures (at 1000mb) are obtained from the surface energy balance equation.

The surface, $H_s(i)$, and the atmospheric, $H_a(i)$, heating processes considered are solar radiation, longwave radiation, convection, evaporation, latent heat release, and oceanic transport. Solar radiation absorbed in the atmosphere and at the earth's surface, $H_a(1)$ and $H_s(1)$, are computed according to Lacis and Hansen (1974), with the modification of cloud albedo being solar zenith angle dependent (see O/A). Clouds are parameterized into an effective single cloud layer with amount, top, base, and optical thickness prescribed from observations. Solar radiation absorbed by H_2O, O_3 are included but not the absorption by O_2, CO_2 and cloud droplets.[1] The distribution of water vapor is determined by assuming fixed vertical profiles and fixed surface relative humidities. Latitudinal variation of total ozone amount is taken from London (after Craig,

[1] O/A added 0.08cm of water vapor to the cloud layer to account for the absorption by cloud droplets. According to our analysis, this only increases the surface temperature by less than 0.1C. Since the liquid water content of the cloud is not well-known, we simply neglect this addition and retain the original Lacis and Hansen routine in this respect.

1965). Solar constant is set to be 1360Wm^{-2} for the standard case, and the annual mean values of cosine solar zenith angle are prescribed to each latitude belt.

Longwave radiation at the earth's surface and its flux divergence in the atmosphere, $H_s(2)$ and $H_a(2)$, are computed according to the emissivity formulation of Sasamori (1968, 1970). The longwave radiative transfer due to CO_2 and H_2O is included, but that due to O_3 is neglected. Both clouds and the earth's surface are assumed to have unit emissivity. The temperature structure for computing longwave radiative flux is assumed to be linear with height for the troposphere and isothermal for the stratosphere. The tropospheric temperature lapse rates are determined from the computed 500mb and surface temperatures. The stratospheric temperatures are set equal to those of the tropopause, and the tropopause heights are fixed to their observed annual mean values. The concentration of CO_2 is assumed to be uniform and taken to be 5×10^{-4} by weight (330×10^{-6} by volume).

The heating of earth's surface by ocean currents, $H_s(5)$, is parameterized according to the diffusivity approach of Sellers (1973), and is computed from the surface temperature gradients. The heating parameterizations modified from O/A are described below.

a. Convection

The sensible heat flux from the earth's surface to the atmosphere through convection and turbulent transfer is parameterized as

$$H_s(3) = -[b\,(T_s - T_5) + c] \tag{1}$$

$$H_a(3) = -H_s(3) \tag{2}$$

where $H_s(3)$ and $H_a(3)$ are surface and atmospheric heating due to convection, respectively, T_s and T_5 are temperatures at 1000mb and 500mb levels, respectively, and b and c are constants independent of latitude. This formulation has been used by Saltzman (1968), Saltzman and Vernekar (1971, 1972), and O/A. The constants b and c used by Saltzman (1968) are determined

from the study of heat budget at 45°N latitude (Saltzman, 1967). O/A adopted Saltzman's suggested value of b but with an adjusted value of c. In this study, Saltzman's suggested value of b, 8.31 cal cm^{-2} day^{-1} K^{-1}, is also adopted. For a fixed value of b, the specification of c generally affects the sensible heat flux, the Bowen ratio, and the tropospheric lapse rate. The constant c used by Saltzman (1968) and O/A are -196.41 and -160 cal cm^{-2} day^{-1}, respectively. It is taken to be -190 and -170 cal cm^{-2} day^{-1} for models A and B, respectively, in order to better simulate the temperature fields.

b. Evaporation

The energy used in evaporating water from the earth's surface, $H_s(4)$, is generally related to the sensible heat flux, $H_s(3)$. Saltzman (1968) assumed that the evaporation (latent heat flux) was linearly proportional to sensible heat flux, with the coefficients prescribed independent of latitude. In model A, we also assumed some kind of relationship exists between latent and sensible heat fluxes. But, the coefficient is determined internally rather than prescribed. In model B, we used the same linear formulation of Saltzman (1968) for evaporation. The parameterizations of evaporation for models A and B, respectively, are

$$H_s(4) = W\, e\, H_s(3) \qquad \text{(model A)}, \tag{3}$$

$$H_s(4) = W\, [e'\, H_s(3) + f'] \qquad \text{(model B)}, \tag{4}$$

where W is a water availability factor depending on the relative amount of ocean, land, sea ice, and snow at each latitude belt, and is assumed to be 1 for ocean, 0.8 for land, and 0 for ice and snow (Saltzman and Vernekar, 1971), e' and f' are constants and taken to be 1.27 and -80.1 cal cm^{-2} day^{-1}, respectively (Saltzman, 1968), and e is determined from the vertical gradients of water vapor and temperature near the earth's surface as

$$e = [L(q_s^* - q_B)]/[c_p(T_s - T_B)]. \tag{5}$$

where q is the specific humidity, T is the temperature, subscripts "s" and "B" refer to the 1000 mb level and the top of the boundary layer, P_B, respectively, q_s^* is the saturated q at 1000 mb, L is the latent heat of condensation, and c_p is the specific heat at constant pressure. In the general circulation models, P_B is usually chosen to be the lowest prognostic level (e.g., Manabe, 1969).

In this study, P_B is specified such that the Bowen ratio of the standard case in each latitude belt is close to its observed value. The coefficient e and the sensible heat flux are determined from the predicted temperature field. Therefore, (3) is a nonlinear relationship between sensible and latent heat flux. For the linear formulation of (4), which is also used by O/A, the relative response of latent and sensible heat to a climatic perturbation is essentially determined by the prescribed constant e'. The ratio of change in latent heat to change in sensible heat due to any perturbation is equal to We'. This ratio is determined by the model when (3) is used.

c. Latent heat release

For an equilibrium condition, latent heat release in an atmospheric column is equal to the latent heat flux from the underneath earth's surface plus the convergence of water vapor by atmospheric circulation. It is assumed in O/A that the flux convergence of water vapor by atmospheric motion is proportional to the deviation of zonally averaged cloud amount from its hemispheric average. Since the cloud amount is fixed in the model, this implies that water vapor flux convergence is independent of atmospheric circulation. According to the cloud statistics of London (1957), this also implies that the latent heat release in the equatorial region (5°N) is very close to the surface evaporation there. These phenomena contradict the observed situation (e.g., Sellers, 1965). Following Sellers (1973), we have computed the flux convergence of water vapor from the computed surface temperature and prescribed vertical profiles of meridional wind and water vapor. The latent heat release, $H_a(4)$, is parameterized by

$$H_a(4) = -H_s(4) - D, \tag{6}$$

where

$$D = \frac{\partial}{a\partial\phi} (M + E), \tag{7}$$

M and E are the mean meridional and eddy transports of water vapor across a latitude circle, respectively, D the flux divergence of moisture, a the radius of the earth, and ϕ the latitude. The vertical profiles of specific humidity, q, and mean meridional wind, v, are assumed, respectively, as

$$q = q_s\,(P/P_s)^{\lambda}, \tag{8}$$

$$v = v_s\,(2P - P_s)/P_s, \tag{9}$$

where P is the pressure and the subscript "s" refers to the 1000mb level. The coefficients of λ are taken from Smith (1966). Note that the same water vapor profiles of (8) are used in the calculations of solar and longwave radiation. The value of q_s is determined from the predicted surface temperatures and the fixed surface relative humidities (Table 2). The mean meridional and eddy transports of water vapor are calculated as

$$M = \frac{\ell L}{g}\int_0^{P_s} v\,q\,dp = \frac{\ell L}{g}\,a_M\,v_s\,q_s\,P_s,$$

$$E = -\frac{\ell L}{g}\int_0^{P_s} K_v\frac{\partial q}{a\partial\phi}\,dp = -\frac{\ell L}{g}\,a_E\,K_v\frac{\partial q_s}{a\partial\phi}P_s,$$

where

$$a_M = \lambda/[(1+\lambda)(2+\lambda)],$$

$$a_E = 1/(1+\lambda),$$

and ℓ is the length of latitude circle, g the acceleration of gravity, K_v is the eddy diffusitivity for water vapor and is assumed as

$$K_v = 0.8\,|\Delta T_s| \times 10^{10}$$

where ΔT_s in the surface temperature difference between successive latitude belts.

The values of v_s can be determined through the equations of motion for the friction layer, by relating the pressure gradient force to the temperature gradient. The zonal (u_s) and meridional (v_s) components of surface wind are written as

$$u_s = 0,\ v_s = \left(\frac{R}{a'}(b-1)\frac{\partial T_s}{a\partial\phi}\right)^{1/2},\ \text{for } \phi = 0$$

$$u_s = [R(b-1)\frac{\partial T_s}{a\partial\phi}]/[f(1+\left|\frac{a'u_s}{f}\right|^3)],\ v_s = a'|u_s|u_s/f,\ \text{for } \phi \neq 0$$

where R is the gas constant, f the coriolis parameter, a' the constant of proportionality relating the frictional force to surface wind speed, and b the constant of proportionality relating the surface pressure gradient force to surface temperature gradient. The values of a' and b are taken from Sellers (1973).

d. Surface albedo

To calculate the surface albedo, the earth's surface is assumed to consist of four surface types, i.e. open ocean, snow free land, snow, and sea ice. The annual mean surface albedo at each latitude is computed as

$$r(\phi) = \sum_{j=1}^{4} \sum_{i=1}^{4} f_j(\phi)\, n_{ij}(\phi)\, r_{ij}(\phi),$$

where i is the index for surface type, j the index for season, $r_{ij}(\phi)$ the reflectivity of surface type i at latitude ϕ during season j, $n_{ij}(\phi)$ the fraction of latitude belt covered by surface type i during season j, and $f_j(\phi)$ the weighting function accounting for the seasonal change in solar radiation that incidences on the earth's surface. The seasonal values of $f_j(\phi)$, shown in Table 3, are computed from the data of Budyko (1963), as analysed by Schutz and Gates (1971, 1972 1973, 1974). Note that the values of $f_j(\phi)$ in O/A are based on solar radiation at the top of the atmosphere. Table 3 also shows the reflectivities of ocean and land, and the observed surface type coverages of Curran et al. (1978). Land reflectivities are taken from Sellers (1973) and vary only with latitude. Ocean reflectivities are taken from Budyko (1974) and vary with latitude and season. The reflectivities of snow and sea ice are made to depend on surface temperature. Following Wetherald and Manabe (1975), sea ice and snow are classified into stable and unstable types. Referring to the surface albedo study of Posey and Clapp (1964), the reflectivities of unstable sea ice and snow are assigned to be 0.4 and 0.5, respectively; those of stable sea ice and snow are 0.6 and 0.7, respectively.

Since the unstable snow/ice is usually associated with higher surface temperature and smaller snow/ice coverage as compared with stable types, the discrimination between the stable and

unstable snow (or sea ice) is made according to the fraction of land covered by snow (or ocean covered by sea ice) in each latitude belt in each season. The critical fraction is taken to be 0.5.

In order to incorporate the feedback mechanism between snow/ice albedo and surface temperature, the snow/ice covers are computed from the model through some empirical relationships between the snow/ice cover and the surface temperature. Since only the annual mean surface temperatures (not the seasonal mean surface temperatures) are computed from the model, the seasonal snow and sea ice covers are related to annual mean surface temperatures. The seasonal linear relationships for snow and sea ice and the data on which they are based are shown in Figs. 1 and 2. These are derived from the surface temperature data of Oort and Rasmusson (1971) and Newell et al. (1972), and the snow/ice cover of Curran et al..

The data of sea ice cover are from the arctic sea ice analyses of the U.S. Navy Fleet Weather Facility for the period of 1972-1975, and those of snow cover are inferred from the satellites of ESSA, ITOS, NOAA, and SMS-1 for the period of 1966-1975. The empirical relationships of Figures 1a, 1c, 2a, and 2c for the winter and summer seasons were made available for Ohring and Adler (1978) to use in their model. Note that the snow and ice covers of spring and fall in O/A are interpolated from those of summer and winter for calculating the mean annual surface albedo. For the experiments with ice-albedo feedback, the seasonal ice and snow covers are computed from the model through these linear relationships, but the observed snow and ice covers (Table 3) are used for the experiments without this feedback mechanism.

e. Cloud parameters

Clouds are parameterized into a single cloud layer, with the amounts the same as in O/A and taken from London (1957). The effective cloud top and base are different from those of O/A. These attitudes are determined from the cloud statistics of London (1957) and Rodgers (1967). We first determined the non-overlapping cloud amount for each cloud type from the cloud amounts of London assuming that clouds were randomly distributed, and then used these non-overlapping cloud amounts as weighting functions to compute the averaged cloud

heights. All clouds are assumed radiatively black. Since the optical properties of Ci cloud are quite different from others, we have subjectively reduced the nonoverlapping cloud amount of Ci by half in determining the effective cloud top and base. As shown in Table 2, the effective cloud top and base are about 1 km lower than those of O/A, and the mean cloud top and base are about 4.7 and 2.7km, respectively.

The optical thickness of the single cloud layer, τ_c, is determined from the six cloud types by considering overlapping clouds. Following Stone et al. (1977), the optical thickness of Ci, As, St, Ns, Cu, and Cb are taken to be 2, 6, 8, 16, 16, and 32, respectively, for determining τ_c of the effective cloud layer. The particulate short wave absorption by cloud droplets and dust is not included. The neglect of absorption by cloud droplets causes an overestimation in single scattering albedo of the cloud. This together with the neglect of short wave absorption by O_2 and CO_2 further causes an overestimation in the planetary albedo and an underestimation in the surface temperature. Therefore, the values of τ_c must be adjusted such that the planetary albedo and surface temperature compare well with the observations. A τ_c of 7 used in O/A appeared to be able to better simulate the observed climate, we have used this value as a reference for adjusting τ_c. The hemispheric mean value of τ_c derived from Stone et al. (1977) is about 11.5, which is 4.5 larger that that used by O/A. In this study, the latitudinal distribution of τ_c derived from Stone et al. is reduced by an amount of 4.5 in each latitude belt. As shown in Table 2, τ_c is smaller in the subtropics and larger in the tropics and the middle latitudes. However, the latitudinal variation in τ_c is small.

3. Simulation of observed climate

For any sensitivity study using a model, it is desirable that the model can reasonably simulate the observed climate. The results of models A and B with the inclusion of ice-albedo feedback and the standard solar constant are compared with the observations in this section. The latitude dependent parameters relating to the heating parameterizations are shown in Tables 2 and 3.

Fig. 3 shows the latitudinal variations and hemispheric mean values of surface (T_s) and 500mb temperature (T_5) for models A and B, together with the observed values from Oort and Rasmusson (1971). The simulated temperatures are in good agreement with the observations for both models, except T_5 at 5°N. The discrepancy of T_5 at the equatorial region between the models and the observations is primarily due to the quasi-geostrophic character of the governing equations. Heat budgets of model atmospheres and those computed from actual atmosphere by London and Sasamori (1971), Sasamori et al. (1972), and Hoyt (1976)[1] are shown in Fig. 4. Heat budget analyses show the following:

(1) The heat budgets are in good agreement between model A and B, except for the energy partition between sensible and latent heat fluxes at the earth's surface.

(2) The radiative energy budgets at the top of the atmosphere are in good agreement between the models and the observations. However, the energy partition between the atmosphere and the earth's surface is different between the models and the observations.

(3) Solar radiation absorbed by the model atmospheres is too small and that absorbed by the model earth's surfaces is too large.

(4) The larger solar radiation absorbed by the model earth's surfaces then induces larger turbulent heat fluxes and net upward IR flux at the model earth's surface.

(5) The larger net upward IR flux at the model earth's surface further induces smaller IR cooling in the model atmospheres.

A comparison of the absorption of solar radiation by absorbers in the atmosphere for model A, model B, and Hoyt (1976) is shown in Table 4. It can be seen that, the smaller absorption of solar radiation by the model atmospheres results primarily from the neglect of absorption

[1] In this study, 'Hoyt (1976)' refers to his cloud model A, which adopted the same cloud statistics of London (1957).

by CO_2, O_2, dust, and cloud droplets. Water vapor and cloud contribute more than half of the difference between absorption by the model atmospheres and that calculated by Hoyt (1976). This difference arises mainly from the different treatment of cloud droplet absorption of solar radiation between Lacis and Hansen (1974) and Hoyt (1976). Short wave absorption by cloud droplets is considered very important according to the latter, but less important according to the former. This discrepancy is quite significant.

Figs. 5 and 6 show the latitudinal distributions of the planetary albedo, surface albedo, solar radiation absorbed by the earth-atmosphere system and outgoing long-wave radiation at the top of the atmosphere for models A and B, together with the values from Hoyt (1976), Ellis and Vonder Haar (1976), and Posey and Clapp (1964). As can be seen from Figs. 5 and 6 that the results of the models are in good agreement with the observations. It is noted that the discrepancy of the outgoing IR flux at the top of the atmosphere between the models and observed values of Ellis and Vonder Haar (1976) reflects the deviation of the computed temperature field. Figs. 7 and 8 show the latitudinal distributions of the absorbed solar radiation and net IR flux at the earth's surface, and the absorbed solar radiation and IR flux divergence in the atmosphere for models A and B, together with the values from Hoyt (1976). Compared to the results of Hoyt (1976), the absorbed solar radiation and net upward IR flux at the earth's surface are larger in the models (Fig. 7), while the absorbed solar radiation and IR flux divergence in the model atmospheres are smaller (Fig. 8).

Latitudinal distributions of the latent and sensible heat fluxes at the earth's surface, and the meridional transport of water vapor and latent heat release in the atmosphere for models A and B, are shown in Figs. 9 and 10, together with the observed values from Sellers (1965) and Starr et al. (1969). As mentioned earlier, the major difference between the heat budgets of models A and B is the energy partition between sensible and latent heat fluxes at the earth's surface. This discrepancy is located in the low latitude (Fig. 9). As a result of a smaller meridional

surface temperature gradient in model A, the magnitude of the meridional transport of water vapor through each latitude circle is slightly smaller in model A than in model B. The divergence of water vapor transport is generally smaller in model A than in model B, but the difference is small. The discrepancy of latent heat release between models A and B is produced by the difference in evaporation at the earth's surface, and is located in the low latitudes (Fig. 10).

In conclusion, the simulated climates are in good agreement between models A and B, with the exception that, in the low latitudes, evaporation is less effective in removing heat from the earth's surface and latent heat release is less effective in heating the atmosphere in model B as compared with model A. Also, the simulated radiative energy budgets at the top of the model atmospheres are in good agreement with the observations. However, the energy partition between the atmosphere and the earth's surface is different between the models and the observations. The neglect of solar absorption by CO_2, O_2, dust, and especially cloud droplets is responsible for this difference in energy partition.

4. Sensitivity to solar constant variations

In order to study the effect of different evaporation parameterizations on climate sensitivity to solar constant variations, several numerical experiments using both models A and B, with and without ice-albedo feedback, were performed for solar constants equal to $0.99S_0$, S_0 and $1.01S_0$. The standard value for solar constant, S_0, is taken to be $1360 Wm^{-2}$. The ice and snow covers are predicted for the cases with ice-albedo feedback, but are fixed to the observed values (Table 3) for the cases without ice-albedo feedback. Tables 5 and 6 show the temperature changes resulting from a 1% change in solar constant for models A and B, and other studies. For the cases without ice-albedo feedback, the magnitude of the temperature changes is essentially symmetric with respect to small changes in solar constant. Therefore, those changes corresponding to a 1% increase in solar constant are not shown in Table 6. As can be seen from Tables 5 and 6, the sensitivity of surface temperature to solar constant variations is much smaller in model

A (nonlinear evaporation formulation) than in model B (linear evaporation formulation). Also, the hemispheric mean surface temperature changes of model B are very close to those of O/A, with a difference of only 0.05°C. With the inclusion of the ice-albedo feedback, the change in surface temperature of model B increases with increasing latitude, which is in agreement with the results of O/A. For the cases without ice-albedo feedback, however, the latitudinal distributions of surface temperature change are different between model B and O/A. The surface temperature changes in O/A decrease with increasing latitude, while the changes in model B are fairly uniform. This is a result of different parameterizations of latent heat release. The flux convergence of water vapor is fixed in O/A, but is predicted in model B. For a reduction in solar constant, although the change in solar input (decreases with increasing latitude) initially tends to produce larger temperature decrease in the low latitude than in the high latitudes. The decreased meridional temperature gradient then causes a reduction of water vapor divergence in the subtropics and of water vapor convergence in the middle and high latitudes. The latent heat release in the atmosphere, in turn, is increased in the subtropics and decreased in the middle and high latitudes. As a result of the change in temperature lapse rate, the turbulent heat flux from the earth's surface to the atmosphere is then decreased in the former and increased in the latter regions. Therefore, the surface temperature change is reduced in the subtropics and is increased in the middle and high latitudes. The mean meridional and eddy transports of water vapor, whose strength depends on the temperature gradient, have an effect of moderating the latitudinal variation of temperature change.

With the inclusion of the ice-albedo feedback mechanism, Table 6 shows that the maximum temperature change occurs at the surface level of the polar region for both models A and B. For the low and middle latitudes, the temperature change is larger at the 500mb level than at the earth's surface for model A, but the reverse is true for model B. The temperature lapse rate is, therefore, decreased in model A and increased in model B for an increase in solar constant. Using a GCM to perform the solar constant experiments, Wetherald and Manabe (1975) found that the

temperature changes are larger at the mid-troposphere than at the earth's surface for the low and middle latitude. This is in agreement with the results of model A. However, contrary to the results of W/M, model A produces the largest temperature change in the stratosphere, which is a result of determining the stratospheric temperatures from the predicted tropospheric temperature lapse rates and fixed tropopause heights. It is expected that the tropopause height determined internally, e.g., through the radiative equilibrium method, might improve these results.

Table 5 shows that the sensitivity of surface temperature change to solar constant variation is the smallest for model A as compared with model B and other studies. In order to investigate the cause of this discrepancy, we have examined the global sensitivity parameters, β, defined by Schneider and Mass (1975) as

$$\beta = S_o \frac{d\bar{T}_s}{dS} = \frac{\bar{F}_o}{(d\bar{F}/d\bar{T}_s) + [(S_o/4)(d\bar{\alpha}/d\bar{T}_s)]},$$

where

$$\bar{F} = \frac{S}{4}(1 - \bar{\alpha}),$$

S is the solar constant, F the outgoing longwave flux, α the planetary albedo, the subscript "o" indicates the standard value, and overbar "–" indicates the global mean. Table 7 shows the results of the global sensitivity parameters for models A and B, and other studies. The major difference between model A and others is the longwave sensitivity parameter $d\bar{F}/d\bar{T}_s$, which is much larger in model A than in other models. It implys that the outgoing longwave radiation is more sensitive to the surface temperature variation in model A than in other models. If we let

$$F = F_1 - (F_i - F_c) A_c,$$

where F_1 and F_c are the outgoing longwave fluxes for clear and overcast skies, respectively, and A_c the cloud amount, the longwave sensitivity parameter may be written as

$$\frac{d\bar{F}}{d\bar{T}_s} = \frac{d\bar{F}_l}{d\bar{T}_s} - \left(\frac{d\bar{F}_l}{d\bar{T}_s} - \frac{d\bar{F}_c}{d\bar{T}_s}\right)\bar{A}_c \qquad \text{for fixed } A_c. \tag{10}$$

Since the cloud amount and height are fixed in the GCM of W/M and models A and B, we have further compared the longwave sensitivity parameters using (10). According to Ramanathan (1977), the results for W/M may be written as

$$\frac{d\bar{F}}{d\bar{T}_s} = \begin{cases} 1.94 + 0.25\,\bar{A}_c & \text{for } S_0 \to S_0 + 2\% \\ 1.8 - 0.4\,\bar{A}_c & \text{for } S_0 \to S_0 - 2\% \end{cases} \text{(W/M)}.$$

The results for models A and B may be written as

$$\frac{d\bar{F}}{d\bar{T}_s} = \begin{cases} 3.84 + 0.12\,\bar{A}_c & \text{for } S_0 \to S_0 + 1\% \\ 3.71 + 0.15\,\bar{A}_c & \text{for } S_0 \to S_0 - 1\% \end{cases} \text{(model A)},$$

and

$$\frac{d\bar{F}}{d\bar{T}_s} = \begin{cases} 2.78 - 0.17\,\bar{A}_c & \text{for } S_0 \to S_0 + 1\% \\ 2.74 - 0.15\,\bar{A}_c & \text{for } S_0 \to S_0 - 1\% \end{cases} \text{(model B)}.$$

As expected, the discrepancy caused by the second term is much smaller than that caused by the first term, and the clear sky longwave sensitivity ($d\bar{F}_l/d\bar{T}_s$) is responsible for the difference in long-wave sensitivity ($d\bar{F}/d\bar{T}_s$). The discrepancy in $d\bar{F}_l/d\bar{T}_s$ between models A and B is mainly due to the difference in the response of the temperature lapse rate to solar constant variations.

As mentioned before, the temperature lapse rate generally decreases in model A and increases in model B as solar constant increases. The outgoing longwave radiation is, therefore, more sensitive to surface temperature change in model A than in model B. On the other hand, the discrepancy in $d\bar{F}_l/d\bar{T}_s$ between model A and W/M comes from the difference in the response of water vapor and the stratospheric temperature to solar constant variation. Although the surface relative humidity is fixed, the relative humidity for the troposphere of models A (and model B) decreases with increasing solar constant. With a 1% increase in solar constant, the relative humidity at 850mb decreases by about 0.8% in model A (about 0.4% in model B). But the results of W/M show that the relative humidity for the lower troposphere increases with increasing

solar constant. Since water vapor is mostly confined to the lower troposphere, this indicates that water vapor must be increased more and the infrared opacity due to water vapor is larger in W/M than in model A to reduce $d\overline{F}/d\overline{T}_S$ as solar constant increases. As mentioned before, the variation in solar constant causes a maximum temperature change in the stratosphere of model A, but a minimum change in the stratosphere of W/M. This also increases the longwave sensitivity parameter in model A as compared to W/M.

The response of surface heat budget to the variation in solar constant for both models are shown in Table 8 and Fig. 11. As can be seen, the responses are quite different due to different parameterizations of evaporation. The results of model A are qualitatively in agreement with those of W/M. Both model A and the GCM of W/M show that the latent heat flux increases with increasing solar constant, but the sensible heat flux decreases with increasing solar constant. As pointed out by Wetherald and Manabe, the nonlinear increase in saturation vapor pressure makes more energy available for evaporation and less energy available for sensible heat flux as the surface temperature increases. Contrary to the results of model A and W/M, the changes in sensible and latent heat in model B are essentially in the same direction due to the linear relationship between them. The difference in the response of sensible heat flux to solar constant variation between models A and B results from the different response in temperature lapse rate, which also produces the difference in the change of the net longwave radiation at the earth's surface. The net longwave radiation changes in model A are much smaller than those of W/M. The response of water vapor to solar constant variation is responsible for this difference. Latent heat flux is more sensitive to solar constant variation for the nonlinear evaporation formulation than for the linear evaporation formulation, with the major difference located in the low latitudes. This implies that cloudiness might be more sensitive to solar constant variation for the case of nonlinear evaporation if clouds are to be generated by the model.

In a reappraisal of the ice-albedo feedback, Lian and Cess (1977) introduced a parameter $\gamma = \beta/\beta' - 1$, to indicate the amplification in global climate sensitivity due to ice-albedo feedback,

where β and β' are the global sensitivity parameters with and without ice-albedo feedback, respectively. The value of γ estimated by them is about 0.25. For the cases with a 1% increase in solar constant, the values of γ in models A and B are about 0.26 and 0.36, respectively. For the cases with a 1% decrease in solar constant, the values of γ are about 0.32 and 0.41 for model A and model B, respectively. The ice-albedo feedback causes an asymetric climate change in both models, with slightly larger amplification for the cases with decreasing solar constant. Although the same parameterization to account for the ice-albedo feedback is used in both models A and B, the amplification factor γ, appears to be smaller in model A than in model B. Also, the values of γ in model A are closer to the results of Lian and Cess (1977) and W/M.

5. Conclusions and remarks

Based upon the annual mean zonally averaged climate model of Ohring and Adler (1978) with some modifications, the effects of different evaporation parameterizations on the climate sensitivity to solar constant variations are investigated. The changes from O/A are the parameterizations of convection, evaporation, latent heat release, cloud properties, and surface albedo. Two different evaporation parameterizations are tested in this study. One is the nonlinear formulation with the Bowen ratio determined by the predicted vertical temperature and humidity gradients near the earth's surface (model A). The other is the linear formulation of Saltzman (1968) with the Bowen ratio essentially determined by the prescribed linear coefficient which is also used in O/A (model B). The major results of this study are summarized below.

1) The computed climates are in good agreement between models A and B, except the energy partition between sensible and latent heat fluxes at the earth's surface. The latent heat flux further induces the difference in latent heat release.

2) The simulated temperatures and the radiation budgets at the top of the atmosphere for both models are in good agreement with the observations, but with different energy partition between the atmosphere and the earth's surface. Compared to the results of Hoyt (1976), the computed atmospheric solar heating and infrared cooling are too small, and the net

solar radiation and the net longwave radiation at the earth's surface are too large. This is a result of neglecting the absorption of solar radiation by CO_2, O_2, dust and cloud droplets in the model.

3) The difference in evaporation parameterizations causes a discrepancy in the response of temperature lapse rate to solar constant variations and a difference in the sensitivity of longwave radiation to surface temperature, $d\bar{F}/d\bar{T}_s$. Compared to the linear evaporation formulation (model B), the nonlinear evaporation formulation (model A) appears to produce a reduction not only in the sensitivity of surface temperature to solar constant variations but also in the amplification of the global climate sensitivity due to ice-albedo feedback.

4) The difference in evaporation also causes a difference in the response of surface heat budget to solar constant variations. The results with the nonlinear evaporation (model A) are qualitatively in agreement with those of Wetherald and Manabe (1975). Both model A and W/M show that the changes of latent and sensible heat fluxes are in the opposite direction, with the latent heat increasing and sensible heat decreasing for an increase in solar constant. The nonlinear increase in saturation vapor pressure makes more energy available for evaporation and less energy available for sensible heat flux as surface temperature increases. However, the responses of sensible and latent heat in model B are in the same direction, and are an outcome of the linear relationship between these fluxes.

5) Latent heat flux is more sensitive to solar constant variation for the nonlinear evaporation than for the linear evaporation, implying that cloudiness might be more sensitive to solar constant variation for the nonlinear evaporation case if clouds are to be generated by the model.

6) Due to the fact that water vapor is determined by fixing vertical lapse rates and surface relative humidities, the lower tropospheric relative humidities in model A (also model B) were found to decrease with increasing solar constant. This is contrary to the results of W/M, in which the lower tropospheric relative humidities increase with increasing solar constant. Therefore, the infrared opacity is smaller in model A than in M/W. For the troposphere of the low

and middle latitudes, the temperature lapse rates decrease with increasing solar constant in both model A and W/M. Since the water vapor increases much less in model A than in W/M as solar constant increases, the increase of downward infrared flux at the earth's surface is smaller in model A than in W/M. Therefore, as the solar constant increases, the decrease of the net infrared flux at earth's surface is smaller in model A than in W/M, and the surface temperature increases less in model A than in W/M. A better method for computing the water vapor is considered crucially important for climate sensitivity studies.

7) Because the stratospheric temperatures in model A are determined from the predicted tropospheric temperature lapse rates and the fixed tropopause heights, the variations in solar constant were found to produce the maximum temperature changes in the stratosphere, which is contrary to the results of W/M. It is expected that if the tropopause height is determined internally e.g., through the radiative equilibrium method, the results might be improved.

8) For a small variation in solar constant, the hemisphere mean surface temperature changes are in good agreement between model B and O/A. The ice-albedo feedback causes the change in surface temperature to increase with increasing latitude in model B and O/A. For the case without ice-albedo feedback, however, the latitudinal distributions of surface temperature changes are different between model B and O/A. The parameterization of latent heat release is responsible for this difference.

References

Budyko, M. I., 1963: Atlas of the heat balance of the earth. Gidrometeorizdat, Moscow. [NTIS No. 78A46579].

_____, 1969: The effect of solar radiation variations on the climate of the earth. Tellus, 21, 611-619.

_____, 1974: Climate and Life. Academic Press, 508 pp.

Cess, R. D., 1976: Climate change: An appraisal of atmospheric feedback mechanisms employing zonal climatology. J. Atmos. Sci., 33, 1831-1843.

Charney, J., W. J. Quirk, S. Chow, and J. Kornfield, 1977: A comparative study of the effects of albedo change on drought in semi-arid regions. J. Atmos. Sci., 34, 1366-1385.

Craig, R. A., 1965: The Upper Atmosphere: Meteorology and Physics, Academic Press, 509 pp.

Curran, R. J., R. Wexler, and M. L. Nack, 1978: Albedo climatology analyses and the determination of fractional cloud cover. NASA Technical Memorandum 79576, 45 pp. (submitted to J. Appl. Meteor.)

Ellis, J. S., and T. H. Vonder Haar, 1976: Zonal average earth radiation budget measurements from satellites for climate studies. Atmos. Sci. Pap. No. 240, Colorado State University, 50 pp. [NTIS No. 77N13588]

Gal-Chen, T., and S. H. Schneider, 1976: Energy balance climate modeling: Comparison of radiative and dynamic feedback mechanisms. Tellus, 28, 108-121.

Green, J. S. A., 1970: Transfer Properties of the large-scale eddies and the general circulation of the atmosphere. Quart. J. R. Met. Soc., 96, 157-185.

Hoyt, D. V., 1976: The radiation and energy budgets of the earth using both ground-based and satellite-derived values of total cloud cover. NOAA Tech. Rep. ERL 362-ARL 4, 124 pp. [NTIS No. 77N12632].

Lacis, A. A., and J. E. Hansen, 1974: A parameterization for the absorption of solar radiation in the earth's atmosphere. J. Atmos. Sci., 31, 118-133.

Lian, M. S., and R. D. Cess, 1977: Energy-balance climate models: A reappraisal of ice-albedo feedback. J. Atmos. Sci., 34, 1058-1062.

London, J., 1957: A study of the atmospheric heat balance. Final Rep., Contract No. AF 19 (122)-165, College of Engineering, Dept. of Meteorology and Oceanography, New York University, 99 pp. [NTIS No. PB115626].

London, J., and T. Sasamori, 1971: Radiative energy budget of the atmosphere, in Man's Impact on Climate, edited by H. Matthews, W. W. Kellogg, and G. D. Robinson, MIT Press, Cambridge, Mass., 141-155.

Manabe, S., 1969: Climate and the ocean circulation. 1. The atmospheric circulation and the hydrology of the earth's surface. Mon. Wea. Rev., 97, 739-774.

_____, and T. T. Wetherald, 1967: Thermal equilbrium of the atmosphere with a given distribution of relative humidity. J. Atmos. Sci., 24, 241-259.

Newell, R. E., J. W. Kidson, D. G. Vincent, and G. J. Boer, 1972: The General Circulation of the Tropical Atmosphere and Interactions with Extra-tropical Latitudes. MIT Press, 258 pp.

Ohring, G., and S. Adler, 1978: Some Experiments with a zonally averaged climate model. J. Atmos. Sci., 35, 186-205.

Oort, A. H., and E. M. Rasmusson, 1971: Atmospheric circulation statistics. NOAA Prof. Pap. 5, 323-pp. [NTIS No. 72N20553].

Posey, J. W., and P. F. Clapp, 1964: Global distribution of normal surface albedo. Geofis. Int. 4, 33-48.

Ramanathan, V., 1977: Interactions between ice-albedo, lapse rate and cloud-top feedback: An analysis of the nonlinear response of a GCM climate model. J. Atmos. Sci., 34, 1885-1897.

Rodgers, C. D., 1967: The radiative heat budget of the troposphere and lower stratosphere. Rep. A2, Dept. of Meteorology, MIT, 99 pp. [NTIS No. 68N19460].

Saltzman, B., 1967: On the theory of the mean temperature of the Earth's surface. Tellus, 19, 219–229.

_____, 1968: Steady state solutions for axially-symmetric climatic variables. Pure Appl. Geophys., 69, 237–259.

_____, and A. D. Vernekar, 1971: An equilibrium solution for the axially symmetric component of the earth's macroclimate. J. Geophys. Res., 76, 1498–1524.

_____, and _____, 1972: Global equilibrium solutions for the zonally averaged macroclimate. J. Geophys. Res., 77, 3936–3945.

Sasamori, T., 1968: The radiative cooling calculation for application to general circulation experiments. J. Appl. Meteor., 7, 721–729.

_____, 1970: Simplification of radiative cooling calculation for application to atmospheric dynamics. WMO Tech. Note 104, 479–488.

_____, J. London, and D. V. Hoyt, 1972: Radiation budget of the southern hemisphere. Meteor. Monogr., No. 35, 9–23.

Schneider, S. H., and C. Mass, 1975: Volcanic dusts, sunspots and temperature trends. Science, 190, 741–746.

Schutz, C., and W. L. Gates, 1971: Global climatic data for surface, 800mb, 400mb: January. The Rand Corporation, R-915-ARPA. [NTIS No. N7222604].

_____, 1972: Global climatic data for surface, 800mb, 400mb: July. The Rand Corporation, R-1029-ARPA. [NTIS No. AD760283].

_____, 1973: Global climatic data for surface, 800mb, 400mb: April. The Rand Corporation. R-1317-ARPA. [NTIS No. 74N32096].

_____, 1974: Global climatic data for surface, 800mb, 400mb: October. The Rand Corporation. R-1425-ARPA. [NTIS No. 74N32081].

Sela, J., and A. Wiin-Nielsen, 1971: Simulation of the atmospheric annual energy cycle. Mon. Wea. Rev., 99, 460–468.

Sellers, W. D., 1965: Physical Climatology. University of Chicago Press, Chicago, 272 pp.

_____, 1973: A new global climatic model. J. Appl. Meteor., 12, 241–254.

Smith, W. L., 1966: Note on the relationship between total precipitable water and surface dew point. J. Appl. Meteor., 5, 726–727.

Starr, V. P., J. P. Peixoto, and R. McKean, 1969: Pole-to-pole moisture conditions for the IGY. Pure and Appl. Geophys. 75, 300–331.

Stone, P. H., S. Chow and W. J. Quirk, 1977: The July climate and a comparison of the January and July climates simulated by the GISS general circulation model. Mon. Wea. Rev., 105, 170–194.

Wetherald, R. T., and S. Manabe, 1975: The effects of changing the solar constant on the climate of a general circulation model. J. Atmos. Sci., 32, 2044–2059.

Wiin-Nielsen, A., and J. Sela, 1971: On the transport of quasi-geostrophic potential vorticity. Mon. Wea. Rev., 99, 447–459.

_____, and H. Fuenzalida, 1975: On the simulation of the axisymmetric circulation of the atmosphere. Tellus, 27, 199–214.

Table 1
Dynamical Model and Heating Processes, $H_s(i)$ and $H_a(i)$ Indicate the Surface and Atmospheric Heating Processes, Respectively

Dyn Model & Heating Processes	Computation Methods
Two-Level Quasi-Geostrophic Model	Sela and Wiin-Nielson (1971)
Solar Radiation, $H_s(1)$, $H_a(1)$	Lacis and Hansen (1974)
Longwave Radiation, $H_s(2)$, $H_a(2)$	Sasamori (1968, 1970)
Convection, $H_s(3)$, $H_a(3)$	Saltzman (1968)
Evaporation, $H_s(4)$	Non-Linear (Model A, This Study) Linear (Model B, Saltzman, 1968)
Latent Heat Release, $H_a(4)$	Sellers (1973)
Ocean Transport, $H_s(5)$	Sellers (1973)
$H_a = \sum_{i=1}^{4} H_a(i)$, $\sum_{i=1}^{5} H_s(i) = 0$	

Table 2
Latitude Dependent Parameters

Parameters	Latitude (°N)									
	0	10	20	30	40	50	60	70	80	90
Cloud Amount, N	0.51	0.44	0.41	0.47	0.57	0.64	0.64	0.61	0.55	
Cloud Top Height, Z_t (km)	5.5	5.3	5.1	4.8	4.3	3.8	3.8	3.2	3.2	
Cloud Base Height, Z_b (km)	2.9	3.1	3.3	3.1	2.5	2.1	1.8	1.7	1.6	
Cloud Optical Thickness, τ_c	7.6	7.1	6.6	6.5	6.8	7.1	7.2	7.0	6.6	
Surface Relative Humidity (%)	83	76	71	72	75	81	88	92	91	
H_2O Vertical Profile Constant, λ	2.92	2.91	3.13	3.00	2.78	2.80	2.42	2.04	1.63	
Boundary Layer Top, P_B (mb)	930	930	930	940	970	985	996	999	999	
a' (10^{-7} cm^{-1})	0.99	1.10	1.42	1.73	1.99	2.26	2.63	1.94	0.62	0.00
b	1.16	1.17	1.19	1.10	0.95	0.86	0.96	1.10	1.16	0.00

Table 3
Parameters for Surface Albedo Calculation

Parameter	Season	Latitude (°N)								
		5	15	25	35	45	55	65	75	85
Land Reflectivity		0.08	0.13	0.18	0.16	0.15	0.16	0.16	0.16	0.16
Ocean Reflectivity	DJF	0.06	0.06	0.08	0.10	0.13	0.17	0.19	0.23	0.23
	MAM	0.06	0.06	0.06	0.07	0.08	0.09	0.11	0.13	0.13
	JJA	0.06	0.06	0.06	0.06	0.07	0.08	0.09	0.10	0.10
	SON	0.06	0.06	0.07	0.08	0.10	0.12	0.14	0.15	0.15
Fraction of Solar Radiation	DJF	0.24	0.23	0.18	0.15	0.11	0.07	0.03	0	0
	MAM	0.27	0.28	0.28	0.29	0.31	0.36	0.38	0.38	0.37
	JJA	0.24	0.75	0.30	0.34	0.38	0.42	0.50	0.57	0.59
	SON	0.25	0.24	0.24	0.22	0.20	0.15	0.09	0.05	0.04
Ocean Fraction	DJF	0.78	0.72	0.62	0.56	0.48	0.37	0.14	0.10	0
	MAM	0.78	0.72	0.62	0.56	0.48	0.37	0.14	0.09	0
	JJA	0.78	0.72	0.62	0.56	0.48	0.42	0.20	0.17	0.01
	SON	0.78	0.72	0.62	0.56	0.48	0.42	0.22	0.26	0.01
Land Fraction	DJF	0.22	0.28	0.38	0.38	0.15	0.05	0.01	0	0
	MAM	0.22	0.28	0.38	0.44	0.37	0.24	0.10	0.01	0
	JJA	0.22	0.28	0.38	0.44	0.52	0.55	0.59	0.12	0.01
	SON	0.22	0.28	0.38	0.44	0.43	0.35	0.28	0.05	0.01
Sea Ice Fraction	DJF	0	0	0	0	0	0.06	0.16	0.61	0.94
	MAM	0	0	0	0	0	0.06	0.16	0.62	0.94
	JJA	0	0	0	0	0	0.01	0.10	0.54	0.93
	SON	0	0	0	0	0	0.01	0.08	0.45	0.92
Snow Fraction	DJF	0	0	0	0.06	0.37	0.52	0.69	0.29	0.06
	MAM	0	0	0	0	0.15	0.33	0.60	0.28	0.06
	JJA	0	0	0	0	0	0.02	0.11	0.17	0.05
	SON	0	0	0	0	0.09	0.22	0.42	0.24	0.06

Table 4
The Absorption of Solar Radiation by Absorbers in the Atmosphere for Models A and B, and Hoyt (1976) Cloud Model A. The Results are Percentages of Solar Radiation Incidence at Top of Atmosphere

	Model A	Model B	Hoyt (1976)
H_2O & Cloud	13.33%	13.48%	17.38%
O_3	3.51%	3.51%	3.40%
CO_2	0	0	0.85%
O_2	0	0	1.70%
Dust	0	0	0.57%
Atm	16.84%	16.99%	23.90%

Table 5
Mean Surface Temperature Changes Resulting from a 1% Change in Solar Constant for Models A and B, Together with the Results from Other Studies (K)

Investigator	No Ice Feedback	Ice Feedback	
	$S_0 \pm 1\%$	$S_0 + 1\%$	$S_0 - 1\%$
Model A	±0.66	+0.82	-0.86
Model B	±1.03	+1.40	-1.45
Ohring and Adler (1978)	±0.99	+1.35	-1.50
Gal-Chen and Schneider (1976)	±1.4		-3.1 to -5.4
Sellers (1973)		+0.9	-5
Budyko (1969)	±1.5		-5
Manabe and Wetherald (1967)	±1.3		
Wetherald and Manabe (1975)		+1.5	-2.2

Table 6
Latitudinal Distributions of Temperature Changes at 500mb and 1000mb Levels due to a 1% Change in Solar Constant for Models A and B (K)

P (mb)	Latitude (°N)	Model A			Model B		
		No Ice Feedback	Ice Feedback		No Ice Feedback	Ice Feedback	
		-1%	+1%	-1%	-1%	+1%	-1%
500	5	-0.9	0.9	-1.0	-1.0	1.2	-1.2
	15	-0.8	0.9	-0.9	-0.9	1.0	-1.0
	25	-0.8	0.9	-0.9	-0.8	1.0	-1.0
	35	-0.8	0.9	-1.0	-0.8	1.2	-1.2
	45	-0.8	1.1	-1.2	-0.9	1.5	-1.6
	55	-0.8	1.2	-1.3	-1.0	1.7	-1.8
	65	-0.8	1.3	-1.3	-1.0	1.8	-1.9
	75	-0.8	1.3	-1.4	-1.0	2.0	-2.0
	85	-0.8	1.4	-1.4	-1.0	2.1	-2.2
	Mean	-0.79	1.01	-1.05	-0.91	1.30	-1.36
1000	5	-0.7	0.8	-0.8	-1.1	1.2	-1.3
	15	-0.7	0.7	-0.7	-1.0	1.2	-1.2
	25	-0.6	0.7	-0.7	-1.0	1.2	-1.2
	35	-0.6	0.7	-0.7	-1.0	1.2	-1.3
	45	-0.6	0.8	-0.8	-1.0	1.3	-1.3
	55	-0.6	0.9	-0.9	-1.0	1.5	-1.6
	65	-0.7	1.2	-1.2	-1.0	2.0	-2.3
	75	-0.8	1.4	-1.7	-1.0	2.9	-3.0
	85	-0.8	2.1	-2.5	-1.1	2.7	-2.2
	Mean	-0.66	0.82	-0.86	-1.03	1.40	-1.45

Table 7
Global Sensitivity Parameters for Models A and B, and Other Studies (Wm^{-2} K^{-1})

	No Ice Feedback			Ice Feedback					
	$S_0 \pm 1\%$			$S_0 + 1\%$			$S_0 - 1\%$		
	$\frac{d\bar{F}}{d\bar{T}_s}$	$\frac{S_0}{4}\frac{d\bar{\alpha}}{d\bar{T}_s}$	$\frac{d\bar{\alpha}}{d\bar{T}_s}$	$\frac{d\bar{F}}{d\bar{T}_s}$	$\frac{S_0}{4}\frac{d\bar{\alpha}}{d\bar{T}_s}$	$\frac{d\bar{\alpha}}{d\bar{T}_s}$	$\frac{d\bar{F}}{d\bar{T}_s}$	$\frac{S_0}{4}\frac{d\bar{\alpha}}{d\bar{T}_s}$	$\frac{d\bar{\alpha}}{d\bar{T}_s}$
Model A	3.82	-0.25	-0.0007	3.91	-1.05	-0.0031	3.79	-1.09	-0.0032
Model B	2.52	-0.24	-0.0007	2.70	-1.02	-0.0030	2.67	-1.05	-0.0031
Budyko (1969)	1.45	0	0						
Cess (1976)	1.63	-0.10	-0.0003						
Wetherald and Manabe (1975)				2.07	-0.52	-0.0015	1.60	-0.54	-0.0016

Table 8
Percentage Changes of Surface Heat Budget Components Resulting from the Changes in Solar Constant for both Models A and B (with Ice Feedback). SR, Solar Radiation Absorbed at the Earth's Surface; LR, Net Upward Longwave Radiation at the Earth's Surface; SH, Upward Flux of Sensible Heat at the Earth's Surface; LH, Upward Flux of Latent Heat at the Earth's Surface; W/M, General Circulation Model of Wetherald and Manabe (1975). Numbers in Parentheses Indicate the Hemispheric Mean Surface Heat Budget for the Standard Cases (w m^{-2})

	Model A			Model B			W/M		
	$0 \rightarrow 1\%$	$0 \rightarrow -1\%$		$0 \rightarrow 1\%$	$0 \rightarrow -1\%$		$0 \rightarrow 2\%$	$0 \rightarrow -2\%$	$-2\% \rightarrow -4\%$
SR (176.8)	+1.2%	-1.2%	(176.0)	+1.3%	-1.3%	(166.0)	+1.7%	-2.1%	-2.9%
LR (67.1)	-0.2%	+0.1%	(67.8)	+0.4%	-0.4%	(63.5)	-4.4%	+2.2%	+2.2%
SH (26.4)	-2.9%	+2.9%	(37.3)	+1.1%	-1.0%	(27.2)	-5.1%	+0%	+7.7%
LH (83.3)	+3.5%	-3.6%	(70.9)	+2.1%	-2.3%	(75.3)	+9.3%	-6.5%	-10.2%

FIGURE CAPTIONS

Figure

1 Relationships Between Seasonal Snow Cover over Land and the Mean Annual Surface Temperature

2 Relationships Between Seasonal Ice Cover over Ocean and the Mean Annual Surface Temperature

3 Latitudinal Distributions of Surface (T_s) and 500mb Temperatures (T_5) for Models A and B, Together with the Observed Values from Oort and Rasmusson (1971)

4 Heat Budgets of Model Atmospheres, and those Computed from Actual Atmosphere by London and Sasamori (1971), Sasamori et al. (1972), and Hoyt (1976)

5 Latitudinal Distributions of the Planetary Albedo (a), and the Surface Albedo (b) for Models A and B, Together with the Values from Hoyt (1976), Ellis and Vonder Haar (1976) and Posey and Clapp (1964)

6 Latitudinal Distributions of the Solar Radiation Absorbed by Earth–Atmosphere System (a), and the Outgoing Longwave Radiation at the Top of Atmosphere (b), for Models A and B, Together with the Observed Values from Ellis and Vonder Haar (1976)

7 Latitudinal Distributions of the Solar Radiation Absorbed (a), and the Net IR Flux (b), at the Earth's Surface for Models A and B, Together with the Values from Hoyt (1976)

8 Latitudinal Distributions of the Solar Radiation Absorbed (a), and IR Flux Divergence (b), in the Atmosphere for Models A and B, Together with the Values from Hoyt (1976)

9 Latitudinal Distributions of the Latent Heat Flux (a), and the Sensible Heat Flux (b), at the Earth's Surface for Models A and B, Together with the Observed Values from Sellers (1965)

FIGURE CAPTIONS (Continued)

Figure

10 Latitudinal Distributions of the Meridional Transport of Water Vapor (a), and Latent Heat Release (b), in the Atmosphere for Models A and B, Together with the Observed Values from Starr et al. (1969) and Sellers (1965)

11 Latitudinal Distributions of Surface Heat Budget Changes due to a 1% Decrease in Solar Constant for Models A and B. SR, Solar Radiation Absorbed; LR, Net Upward Long-wave Radiation; SH, Sensible Heat Flux; LH, Latent Heat Flux; OCEAN, Heating due to Oceanic Transport

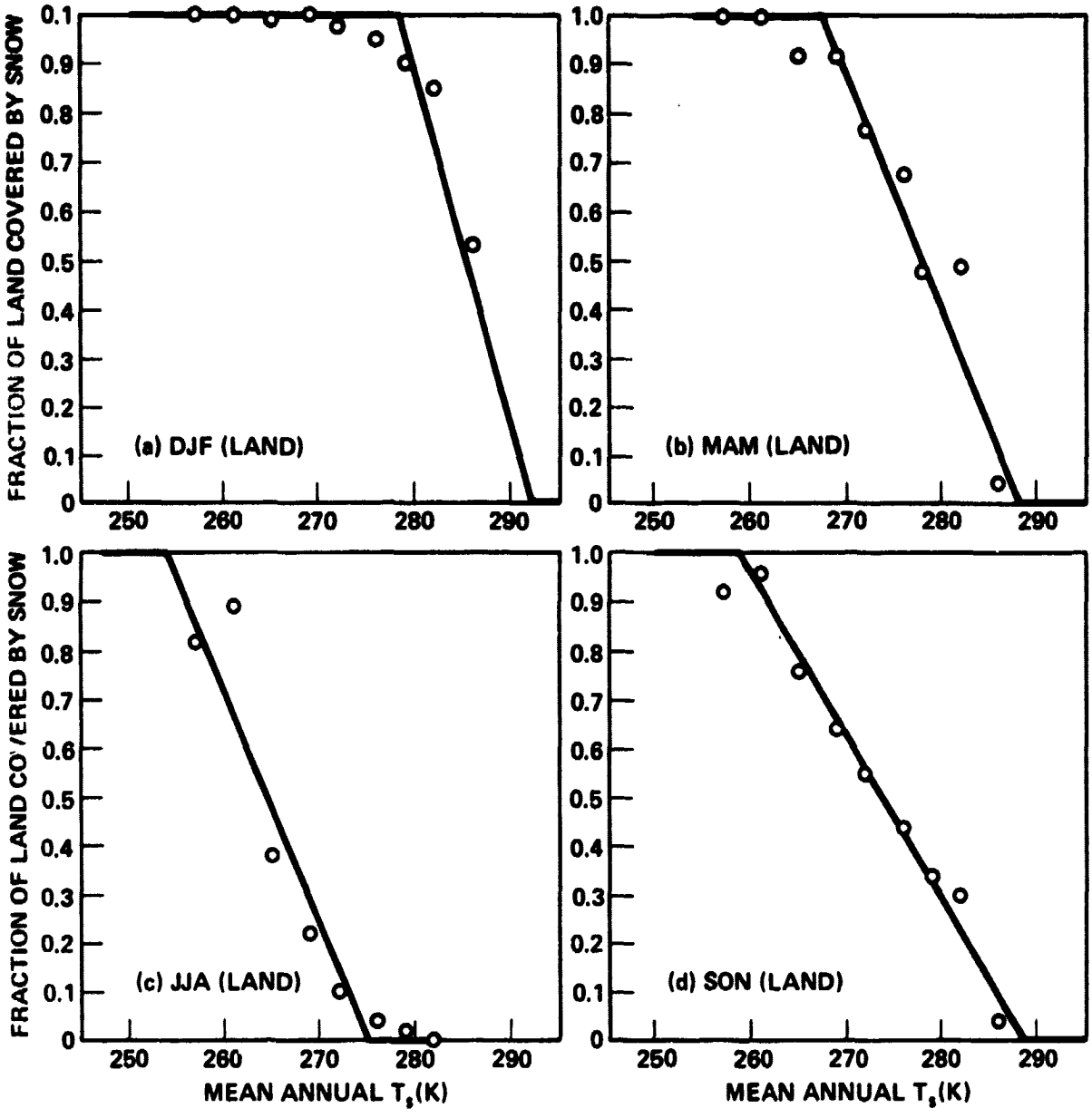

Figure 1. Relationships Between Seasonal Snow Cover over Land and the Mean Annual Surface Temperature

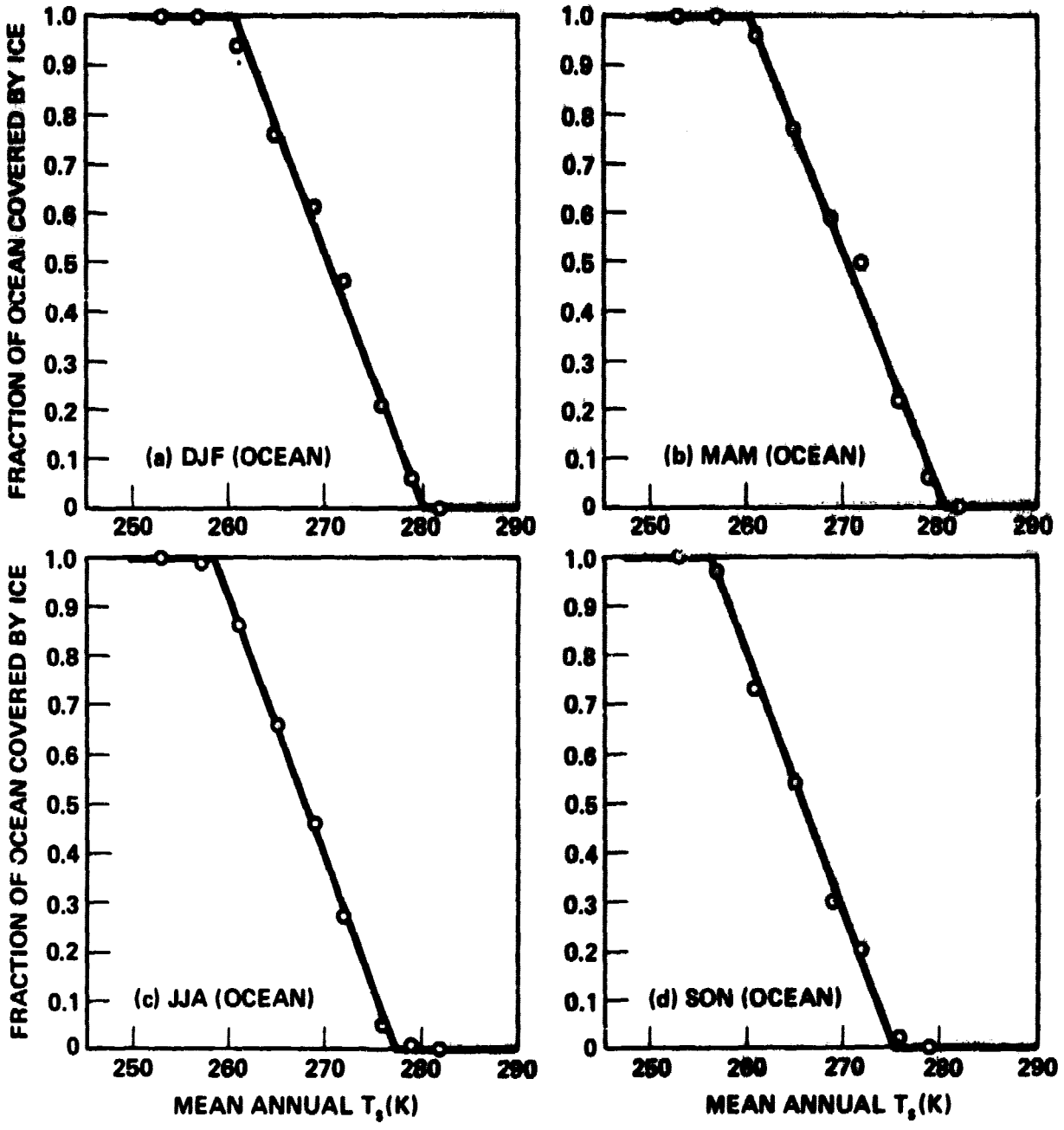

Figure 2. Relationships Between Seasonal Ice Cover over Ocean and the Mean Annual Surface Temperature

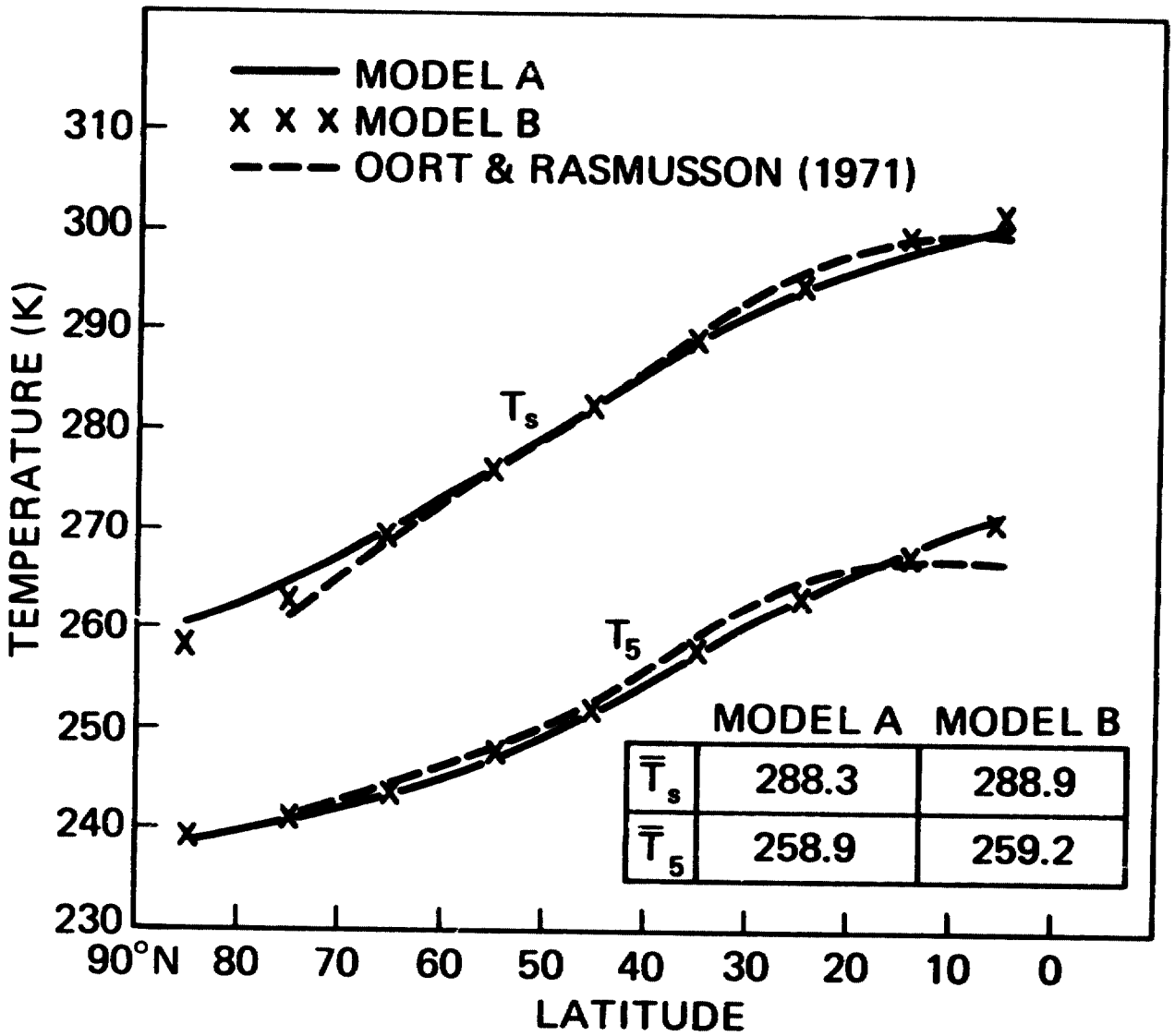

Figure 3. Latitudinal Distributions of Surface (T_s) and 500 mb Temperatures (T_5) for Models A and B, Together with the Observed Values from Oort and Rasmusson (1971)

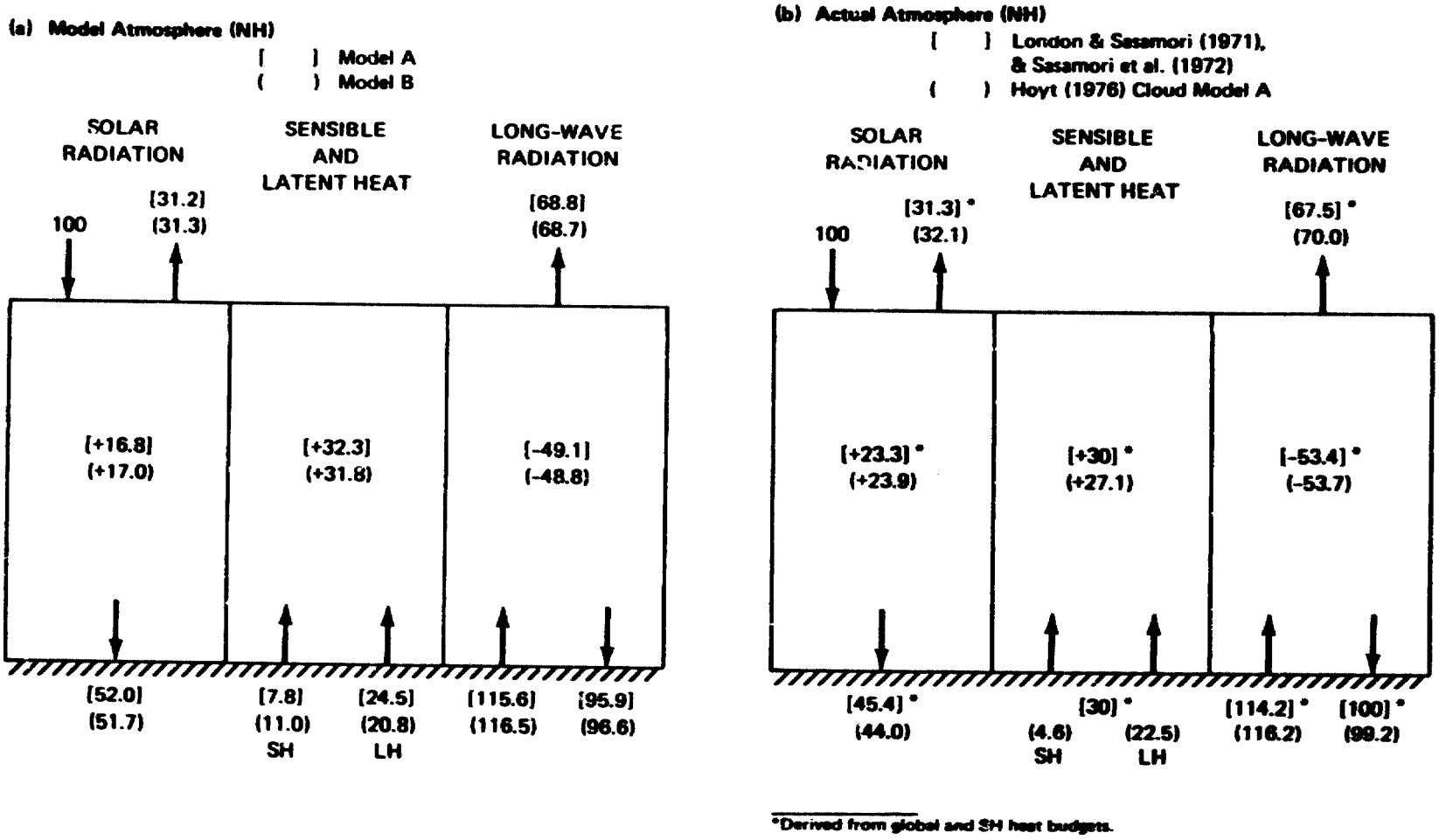

Figure 4. Heat Budgets of Model Atmospheres, and those Computed from Actual Atmosphere by London and Sasamori (1971), Sasamori et al. (1972), and Hoyt (1976)

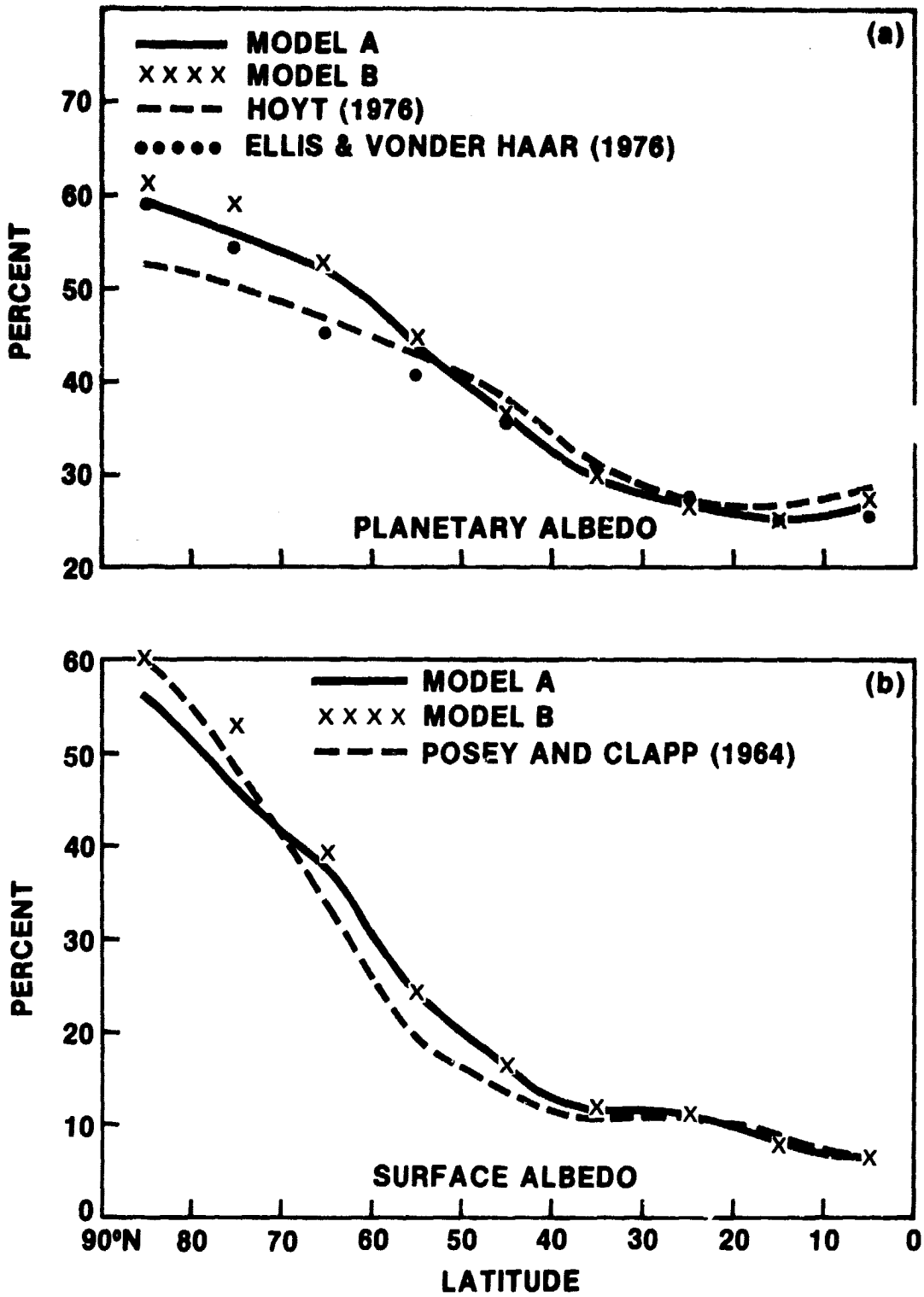

Figure 5. Latitudinal Distributions of the Planetary Albedo (a), and the Surface Albedo (b) for Models A and B, Together with the Values from Hoyt (1976), Ellis and Vonder Haar (1976), and Posey and Clapp (1964)

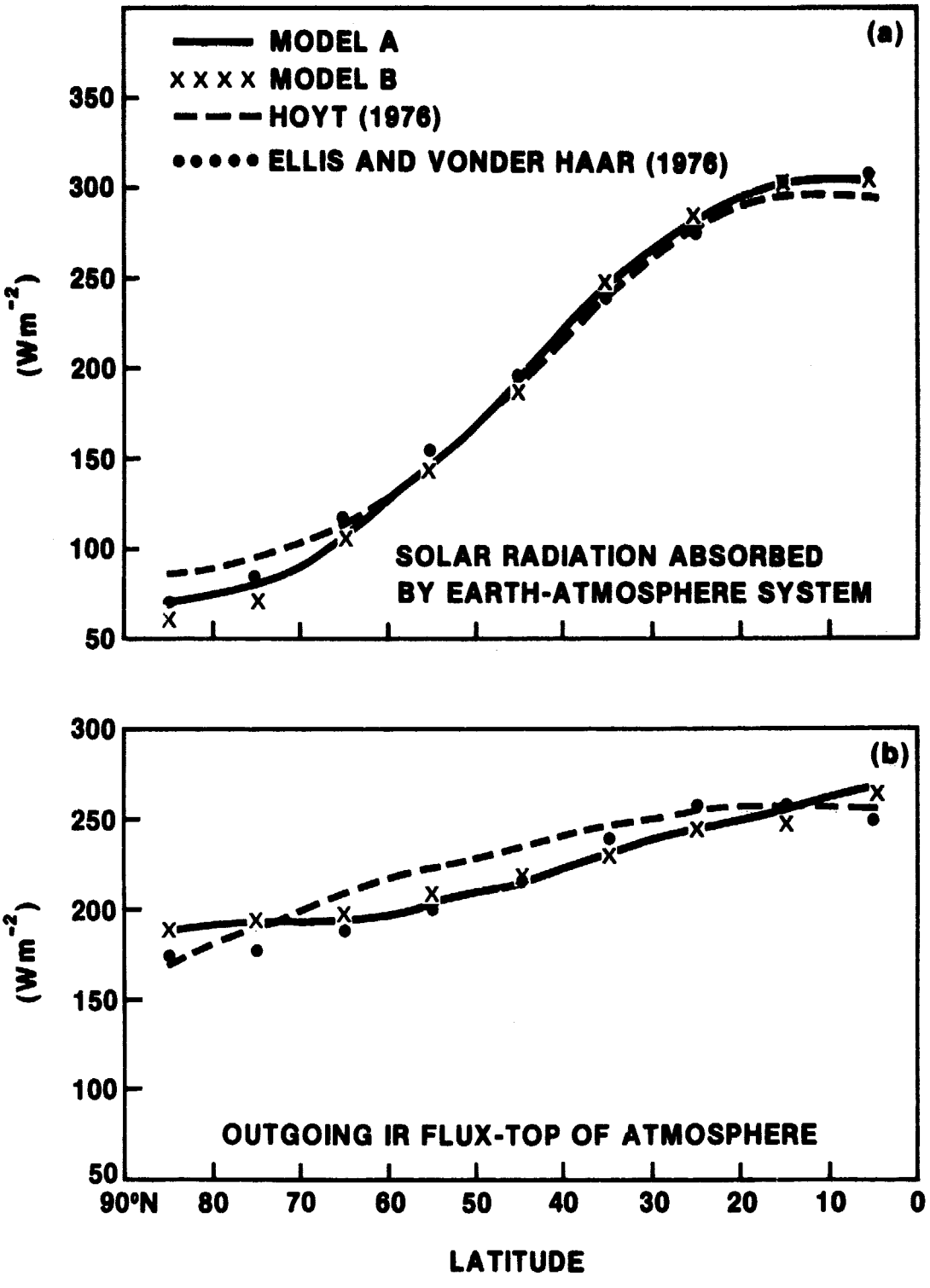

Figure 6. Latitudinal Distributions of the Solar Radiation Absorbed by Earth-Atmosphere System (a), and the Outgoing Long-wave Radiation at the Top of Atmosphere (b), for Models A and B, Together with the Observed Values from Ellis and Vonder Haar (1976)

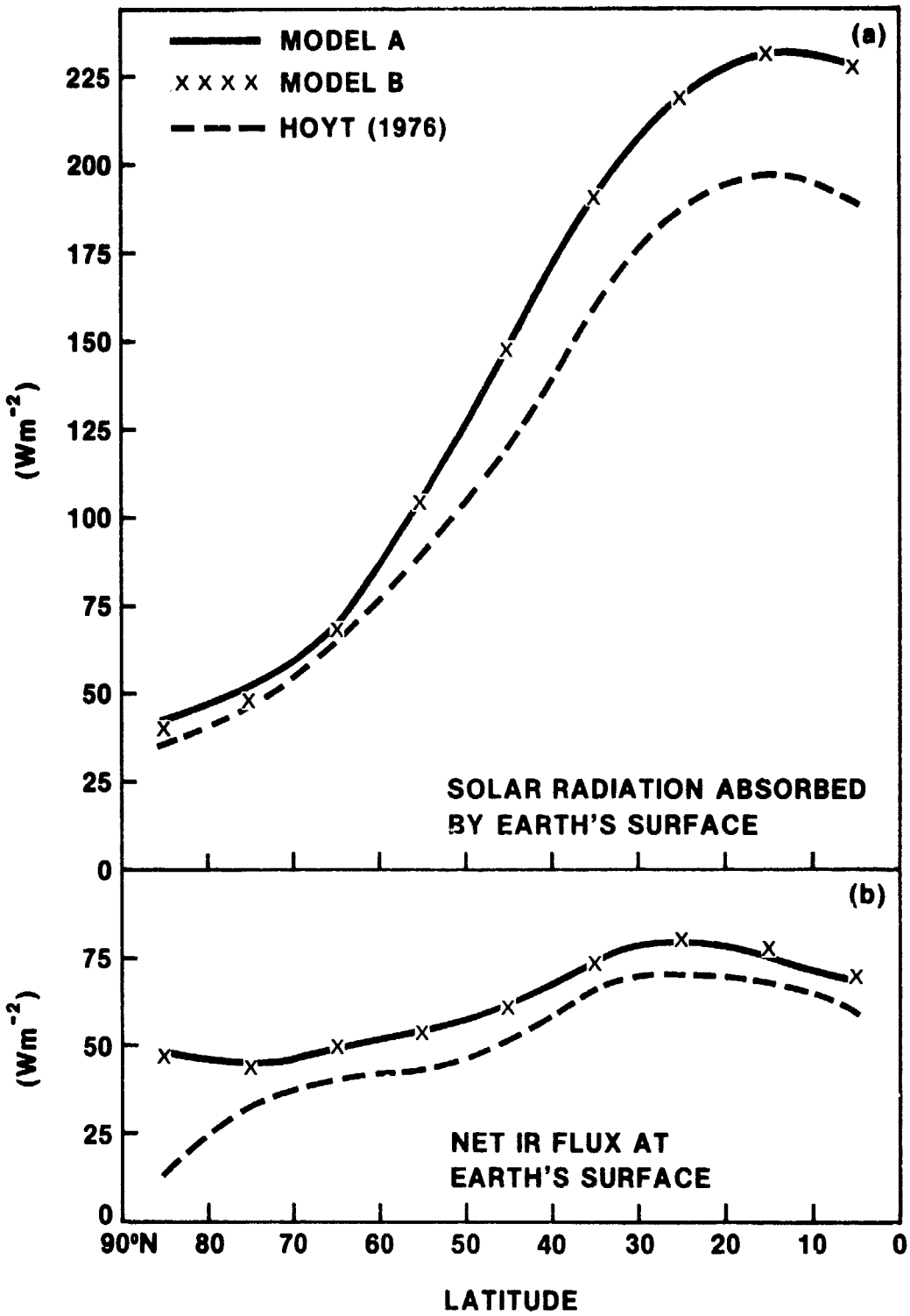

Figure 7. Latitudinal Distributions of the Solar Radiation Absorbed (a), and the Net IR Flux (b), at the Earth's Surface for Models A and B, Together with the Values from Hoyt (1976)

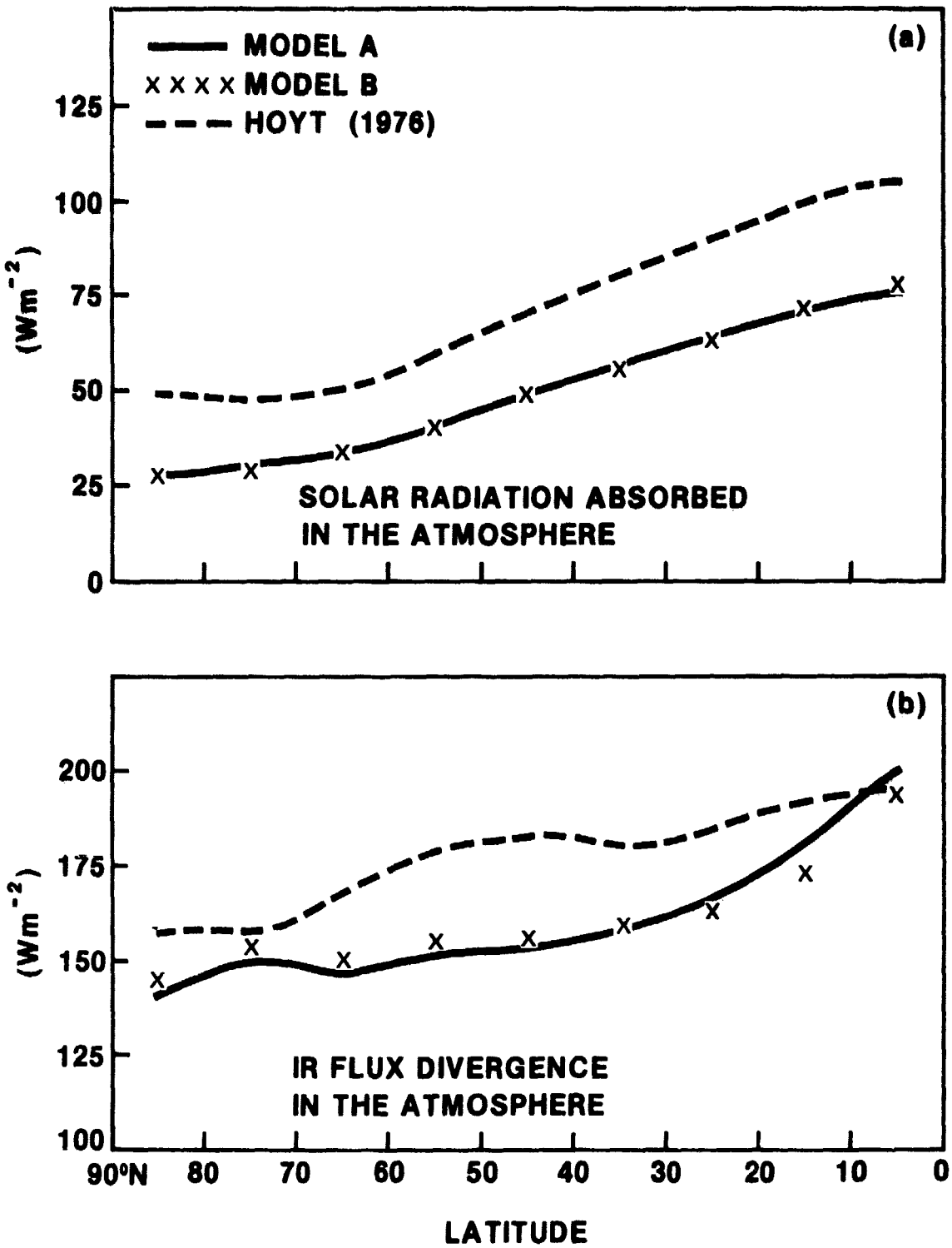

Figure 8. Latitudinal Distributions of the Solar Radiation Absorbed (a), and IR Flux Divergence (b), in the Atmosphere for Models A and B, Together with the Values from Hoyt (1976)

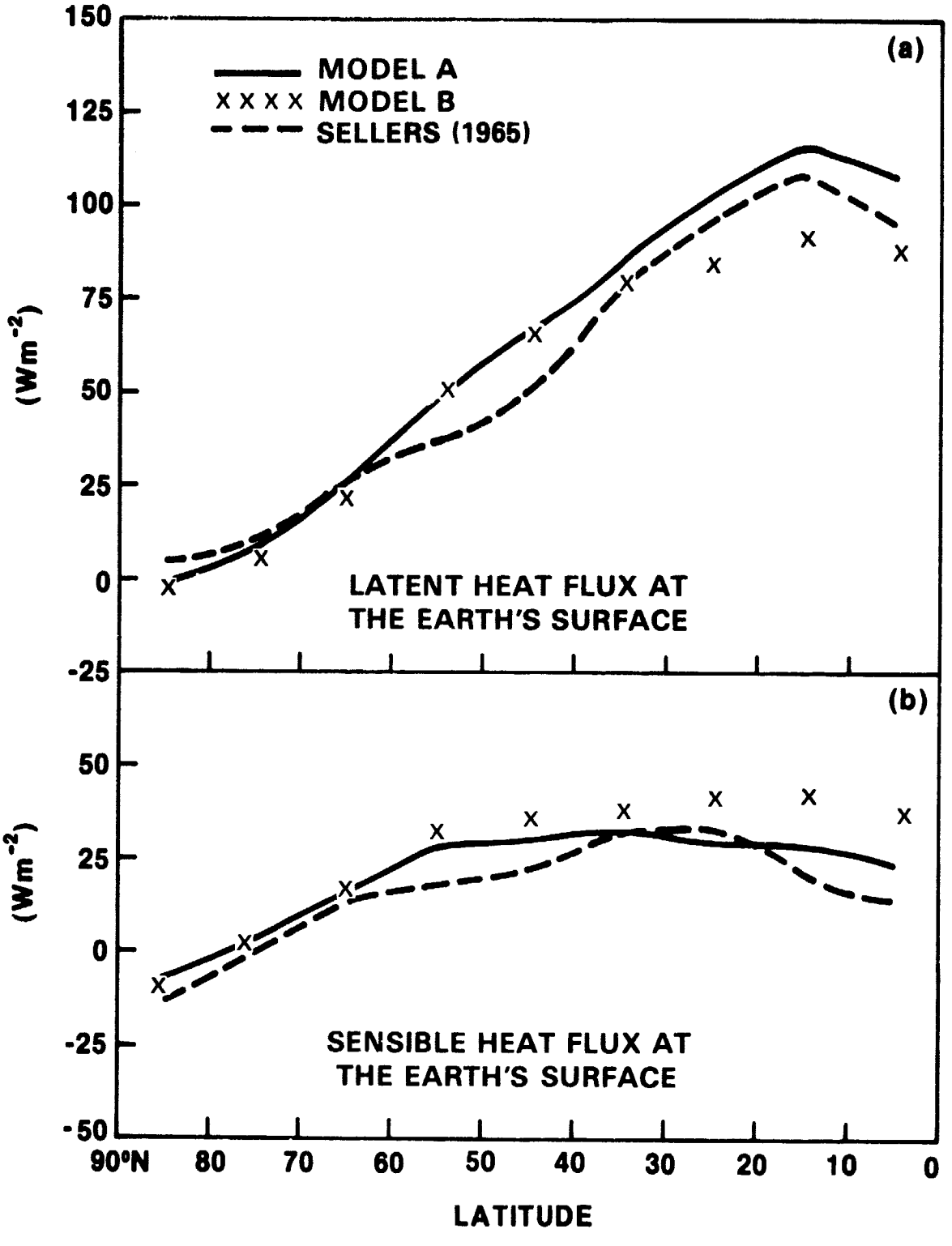

Figure 9. Latitudinal Distributions of the Latent Heat Flux (a), and the Sensible Heat Flux (b), at the Earth's Surface for Models A and B, Together with the Observed Values from Sellers (1965)

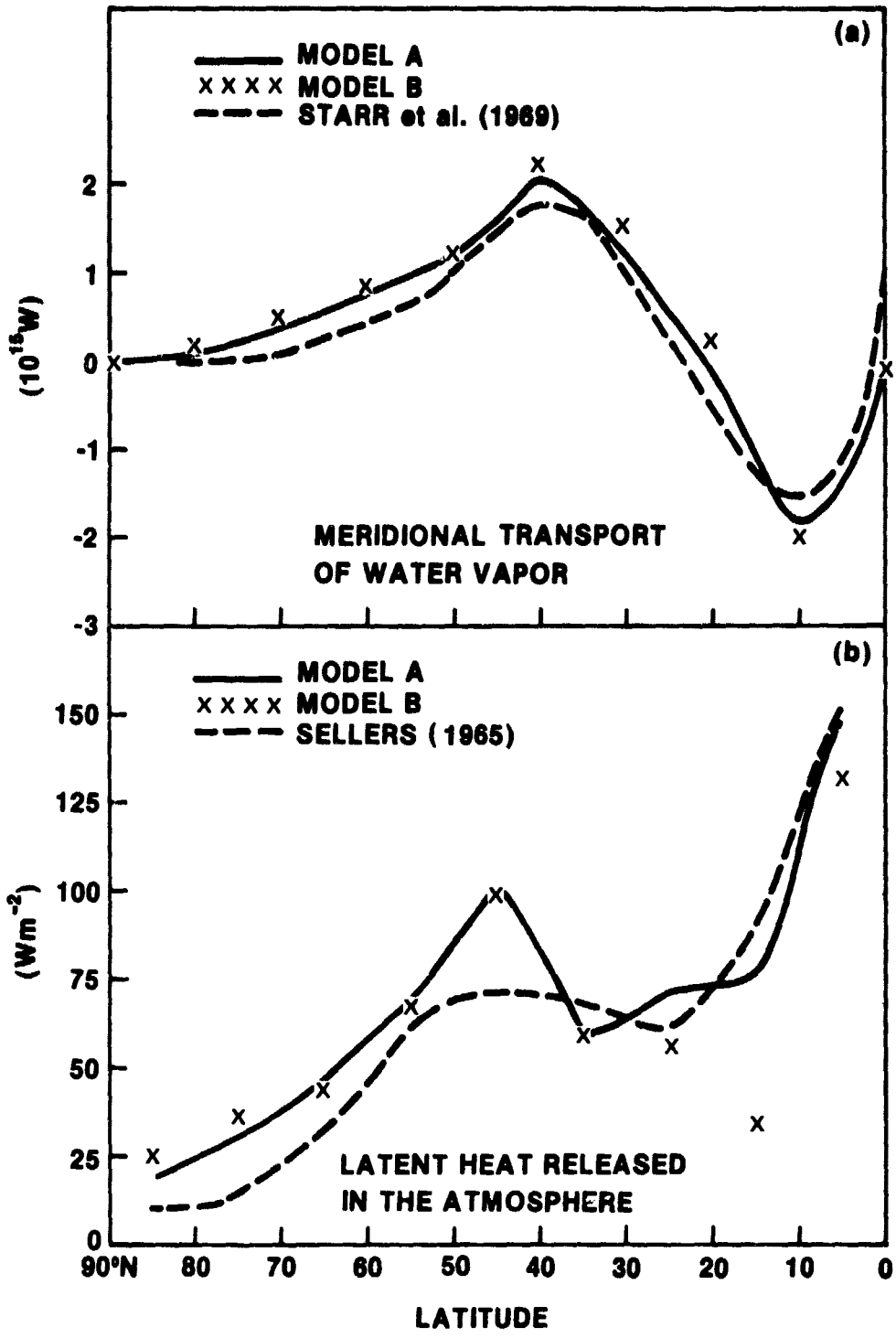

Figure 10. Latitudinal Distributions of the Meridional Transport of Water Vapor (a), and Latent Heat Release (b), in the Atmosphere for Models A and B, Together with the Observed Values from Starr et al. (1969) and Sellers (1965)

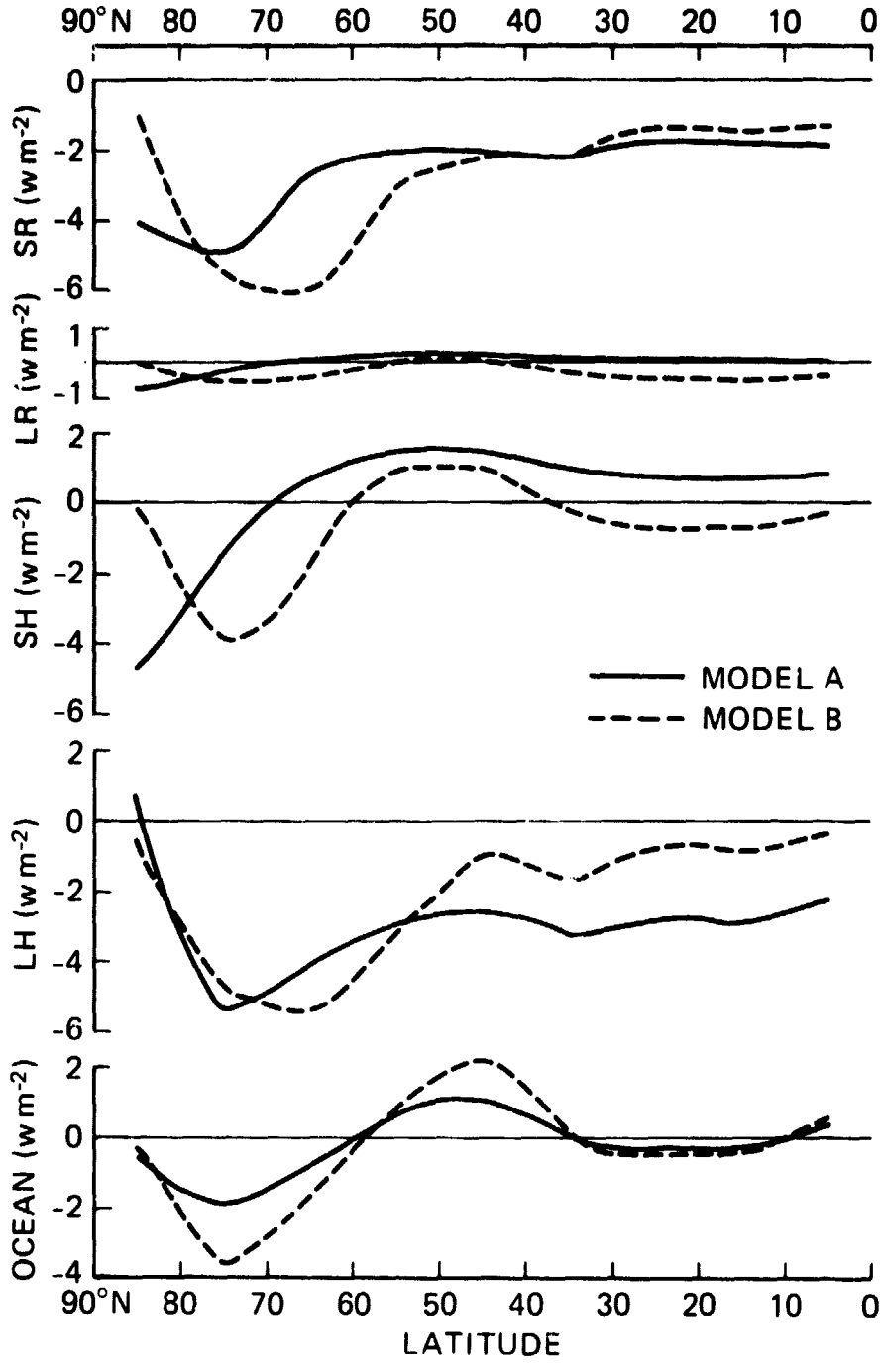

Figure 11. Latitudinal Distributions of Surface Heat Budget Changes due to a 1% Decrease in Solar Constant for Models A and B. SR, Solar Radiation Absorbed; LR, Net Upward Long-wave Radiation; SH, Sensible Heat Flux; LH, Latent Heat Flux; OCEAN, Heating due to Oceanic Transport

BIBLIOGRAPHIC DATA SHEET

1. Report No. 79705	2. Government Accession No.	3. Recipient's Catalog No.
4. Title and Subtitle THE EFFECTS OF GROUND HYDROLOGY ON CLIMATE SENSITIVITY TO SOLAR CONSTANT VARIATIONS		5. Report Date January 1979 6. Performing Organization Code Code 915
7. Author(s) Shu-Hsien Chou, Robert J. Curran, George Ohring		8. Performing Organization Report No.
9. Performing Organization Name and Address Laboratory for Atmospheric Sciences (GLAS) Goddard Space Flight Center Greenbelt, MD 20771		10. Work Unit No. 11. Contract or Grant No. 13. Type of Report and Period Covered Technical Memorandum (Preprint)
12. Sponsoring Agency Name and Address Laboratory for Atmospheric Sciences (GLAS) Goddard Space Flight Center NASA/Goddard Space Flight Center Greenbelt, MD 20771		14. Sponsoring Agency Code

15. Supplementary Notes

The effects of two different evaporation parameterizations on the climate sensitivity to solar constant variations are investigated by using a zonally averaged climate model. The model

16. Abstract

The effects of two different evaporation parameterizations on the climate sensitivity to solar constant variations are investigated by using a zonally averaged climate model. The model is based on the two-level quasi-geostrophic zonally averaged annual mean model of Ohring and Adler (1978) with some modifications to the heating parameterizations. One of the evaporation parameterizations tested is a nonlinear formulation with the Bowen ratio determined by the predicted vertical temperature and humidity gradients near the earth's surface (model A). The other is the linear formulation of Saltzman (1968) with the Bowen ratio essentially determined by the prescribed linear coefficient (model B).

The computed climates are in good agreement between model A and model B, except for the energy partition between sensible and latent heat at the earth's surface. The simulated temperatures and the radiation quantities at the top of the atmosphere for both models are in good agreement with the observations, but the energy partitions between the atmosphere and the earth's surface are different. Compared to the results of Hoyt (1976), the solar heating and the long-wave cooling in the model atmospheres are too small, and the net solar and the net long-wave radiation at the model earth's surfaces are too large. As a result, the turbulent heat flux is too large. The neglect of short wave absorption by CO_2, O_2, dust, and cloud droplets is responsible for this discrepancy.

The surface temperature is less sensitive to solar constant variations and ice-albedo feedback in model A than in model B. The responses of the tropospheric temperature lapse rate and the surface heat budget to solar constant variations are different between these two models. The results of model A are qualitatively in agreement with those of Wetherald and Manabe (1975).

17. Key Words (Selected by Author(s))	18. Distribution Statement
Climate, Hydrology, Solar Constant, Climate Model	

19. Security Classif. (of this report)	20. Security Classif. (of this page)	21. No. of Pages	22. Price*
Nonclassified	Nonclassified		

*For sale by the National Technical Information Service, Springfield, Virginia 22151.

GSFC 25-44 (10/77)